Reprinted from MONTHLY WEATHER REVIEW, Vol. 124, No. 7, July 1996
American Meteorological Society

Impact of Assimilations of Dropwindsonde Data and SSM/I Rain Rates on Numerical Predictions of Hurricane Florence (1988)

JAINN JONG SHI

Science Applications International Corporation, McLean, Virginia

SIMON CHANG

Naval Research Laboratory, Monterey, California

SETHU RAMAN

Department of Marine, Earth and Atmospheric Sciences, North Carolina State University at Raleigh, Raleigh, North Carolina

(Manuscript received 27 June 1995, in final form 20 November 1995)

ABSTRACT

Numerical experiments were conducted to assess the impact of Omega dropwindsonde (ODW) data and Special Sensor Microwave/Imager (SSM/I) rain rates in the analysis and prediction of Hurricane Florence (1988). The ODW data were used to enhance the initial analysis that was based on the National Meteorological Center/Regional Analysis and Forecast System (NMC/RAFS) 2.5° analysis at 0000 UTC 9 September 1988. The SSM/I rain rates at 0000 and 1200 UTC 9 September 1988 were assimilated into the Naval Research Laboratory's limited-area model during model integration.

Results show that the numerical prediction with the ODW-enhanced initial analysis was superior to the control without ODW data. The 24-h intensity forecast error is reduced by about 75%, landfall location by about 95% (reduced from 294 to 15 km), and landfall time by about 5 h (from 9 to 4 h) when the ODW data were included. Results also reveal that the assimilation of SSM/I-retrieved rain rates reduce the critical landfall location forecast error by about 43% (from 294 to 169 km) and the landfall time forecast error by about 7 h (from 9 to 2 h) when the NMC/RAFS 2.5° initial analysis was not enhanced by the ODW data. The assimilation of SSM/I rain rates further improved the forecast error of the landfall time by 4 h (from 4 to 0 h) when the ODW data were used. This study concludes that numerical predictions of tropical cyclone can benefit from assimilations of ODW data and SSM/I-retrieved rain rates.

1. Introduction

The current conventional observation networks and assimilation scheme cannot routinely define tropical cyclone structure and reliable steering flows (Bender et al. 1991; Lord 1991; Davidson and Puri 1992). The accurate description of the initial conditions in numerical simulations of the tropical cyclone usually suffers from two main deficiencies. The first is the lack of observational data over tropical oceans. This is an important factor limiting the improvement of numerical model simulations and the accuracy of hurricane track forecasts (Neumann 1981). A reasonably good density and accuracy of observations are required to initialize hurricane models (Anthes 1982). The second is that prediction models do not accurately reproduce the temporal and spatial distribution of latent heating (up to 300 K day^{-1}), which is the major energy source to drive a hurricane circulation and determine its intensity.

Franklin and DeMaria (1992) demonstrated that the Omega dropwindsonde (ODW) data collected during the 1982–89 synoptic flow experiments resulted in highly consistent reductions in track forecast errors in a barotropic track forecast model. In addition, they demonstrated the ability of utilizing all the data available with a scale-controlled objective analysis described by Ooyama (1987). Their results suggest that the collection of the ODW data in the hurricane environment can be a viable, cost-effective means of improving operational hurricane forecasts. Furthermore, Franklin et al. (1993) used the ODW data in a nested objective analysis scheme following Ooyama (1987) and DeMaria et al. (1992) to determine the kinematic structure of Hurricane Gloria (1985). They asserted that the nested analyses of Hurricane Gloria, based on the ODW and Doppler radar data, were the most complete kinematic analyses of a single hurricane constructed to date.

Corresponding author address: Dr. Jainn Jong Shi, Naval Research Laboratory, Code 7335, 4555 Overlook Ave., SW, Washington, DC 20375.
E-mail: shi@metcomp.nrl.navy.mil

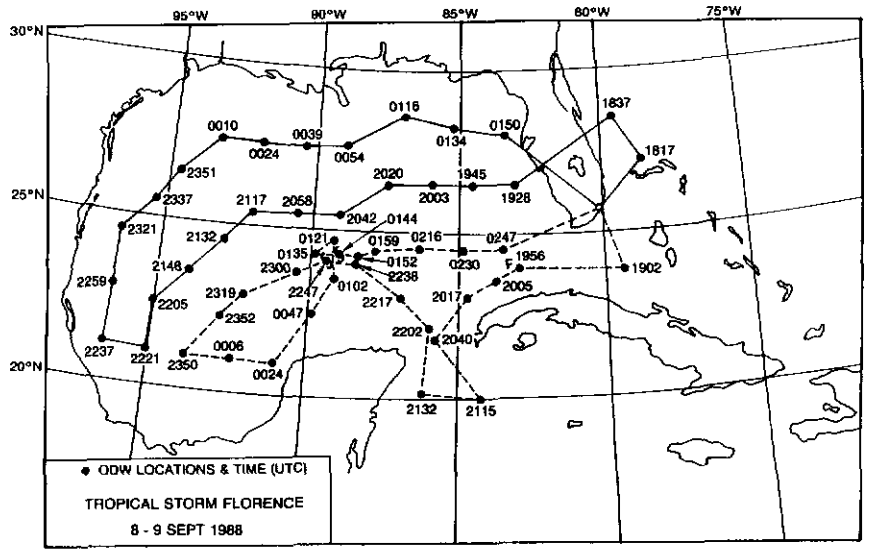

FIG. 1. Location and time (UTC) of the Omega dropwindsonde data collected during the AOML/HRD synoptic flow experiment on 8–9 September 1988.

Despite numerous research efforts, the lack of an accurate reproduction of the temporal and spatial distribution of latent heating remains a major factor contributing to the poor performance in numerical tropical cyclone prediction. Diabatic heat sources, which include latent heating, are generally poorly observed and seldom assimilated in the initial conditions, especially for tropical cyclones (Davidson and Puri 1992). Model forecasted latent heating may not occur in the right place at the right time if the latent heat sources are improperly defined in the initial conditions. Horizontal divergence and moisture fields, crucial variables toward determining the latent heating, are usually poorly analyzed in objective analyses, resulting in the delay of the onset of precipitation or the so-called spinup problem (Chang and Holt 1994). Efforts have been made to assimilate the observed or satellite-retrieved rain rates into numerical models in the past. Molinari (1982) successfully assimilated a relatively small area of radar-observed rain rates into a numerical model to improve the simulation of a hurricane. Idealized rain rates were incorporated into a mesoscale hurricane model by using dynamic initialization (Fiorino and Warner 1981). Chang and Holt (1994) assimilated the Special Sensor Microwave/Imager (SSM/I) rain rates into a limited-area numerical model to simulate a rapidly moving and intensifying extratropical marine cyclone. Their results showed that the assimilation of the SSM/I rain rates cut the intensity forecast error by 50%. These studies have demonstrated that the assimilation of the observed rain rates may have a positive impact on the numerical prediction of tropical and extratropical cyclones.

The primary objective of this study is to investigate the impact of ODW data and the SSM/I rain rates on a numerical prediction of Hurricane Florence (1988). To accomplish this, a research version of the Navy Operational Regional Atmospherical Prediction System (NORAPS) of the Naval Research Laboratory (NRL), which includes an objective analysis, a vertical-mode initialization (VMI) and a limited-area numerical model, will be used.

2. Data sources

The data used for this study were acquired from three different sources: 1) the National Meteorological Center/Regional Analysis and Forecasting System (NMC/RAFS, the NMC is now referred to as the National Centers for Environmental Prediction) 2.5° analyses at 0000 UTC 9 September 1988; 2) the Omega dropwindsonde (ODW) data collected during a synoptic flow experiment (1988) from the Hurricane Research Division (HRD) of the Atlantic Oceanographic and Meteorological Laboratory (AOML) of the National Oceanic and Atmospheric Administration (NOAA); 3) the SSM/I data from the NRL archives. The NMC/RAFS 2.5° analyses were used as the first guess (background data) in the nested-grid analysis scheme that will be discussed in section 5. The ODW data were used to enhance the NMC/RAFS 2.5° analyses. The SSM/I rain rates were assimilated into the numerical model as observational rain rates in the model simulations. The SSM/I data were used for both assimilation and the verification.

Since 1982, synoptic flow experiments have been conducted by the AOML/HRD. The experiments are designed to determine the three-dimensional structure of tropical cyclones below approximately 400 mb from roughly 1000 km of the storm's center out (Kaplan and

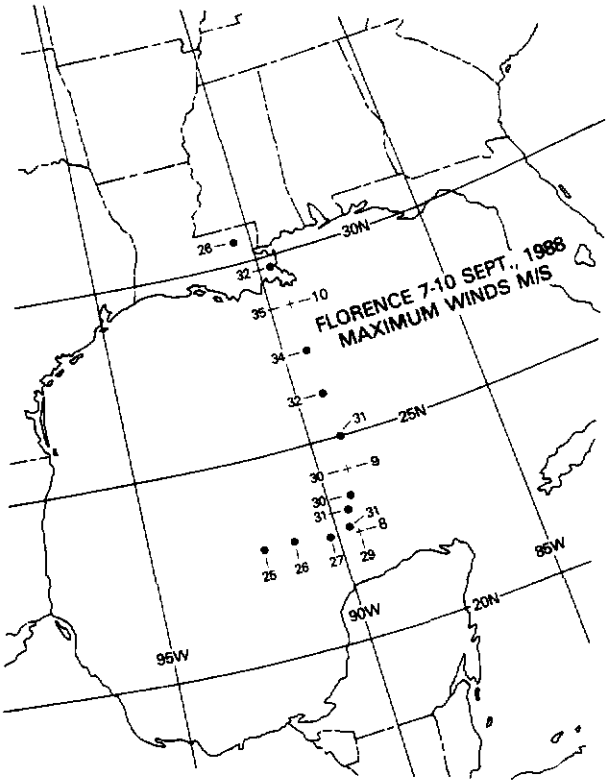

FIG. 2. Position and intensity (maximum winds in meters per second) of Hurricane Florence (7–10 September) every 6 h. Crosses locate Florence's position at 0000 UTC each day. Figure adapted from Rodgers et al. (1991).

Franklin 1991; Franklin et al. 1991; Franklin and DeMaria 1992). During each field experiment, a set of ODW sondes were deployed from NOAA WP-3D aircraft flights at the level near 400 mb over the region surrounding the targeted tropical storm.

A total of 51 ODW datasets were obtained from two NOAA WP-3D aircrafts during the synoptic flow experiment on 8–9 September 1988. These data make a better description of the initial conditions for the numerical simulation of Florence possible. Figure 1 shows the two flight routes and the location and release time of each ODW deployment in the synoptic flow experiment. The release times started at 1817 UTC 8 September 1988 and ended at 0247 UTC 9 September 1988. Each ODW record consisted of the time and location of launch (longitude and latitude), and the sounding data were recorded every 10 mb from the flight level (ranging from 374 to 528 mb) to the surface. The sounding data included pressure, temperature, relative humidity, geopotential height, wind direction, wind speed, and wind uncertainty. The wind data were missing in the lowest few levels near the surface in every ODW record.

Onboard Defense Meteorological Satellite Program (DMSP) satellites, SSM/I is a seven-channel, four-frequency, linearly polarized, passive radiometric system that measures upwelling microwave radiation from the atmosphere and the surface of the earth at 19.3, 22.0, 37.0, and 85.5 GHz (Hollinger 1989 and 1991; Ferriday and Avery 1994). Recent studies (Velden et al. 1989; Rodgers et al. 1991; Alliss et al. 1992, 1993; Chang et al. 1993; Rodgers et al. 1994; Chang and Holt 1994; Rao and MacArthur 1994) have validated the usefulness of the meteorological parameters derived from the SSM/I brightness temperature data for observational and numerical studies. Goerss and Phoebus (1992) reported the operational use of SSM/I wind speed in the Navy Operational Global Atmospheric System (NOGAPS). Chang et al. (1993) found that the SSM/I-retrieved precipitation patterns are very useful in subjective analysis over data-sparse oceans. The SSM/I rain rates used in this study were derived from three SSM/I passes over Florence at 0000 UTC and 1200 UTC 9 September and 0000 UTC 10 September 1988, based on the algorithm described in Hollinger (1991).

3. Synoptic review of Hurricane Florence (1988)

Figure 2, adapted from Rodgers et al. (1991), shows Florence's position and intensity (maximum wind in meters per second) every 6 h between 0600 UTC 7 September and 1200 UTC 10 September 1988. Hurricane Florence's circulation developed from a quasi-stationary frontal cloud band in the south-central Gulf of

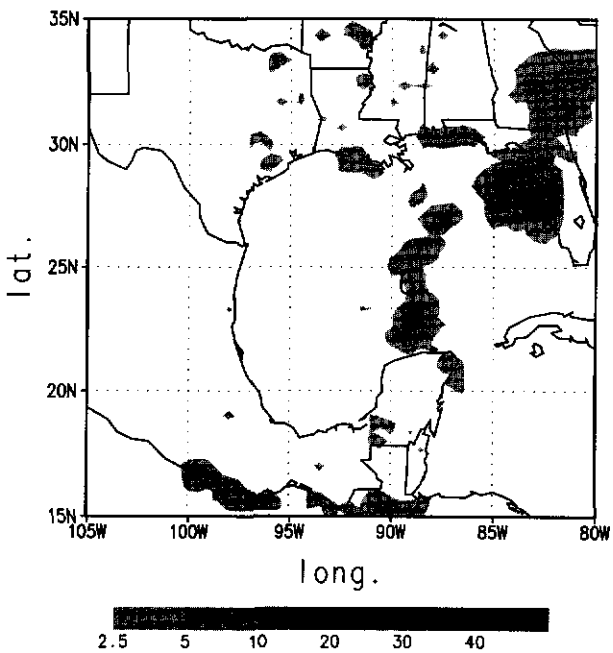

FIG. 3. SSM/I-retrieved rain rates (mm h^{-1}) at 0000 UTC 9 September. The hurricane symbol depicts the location of Florence's center.

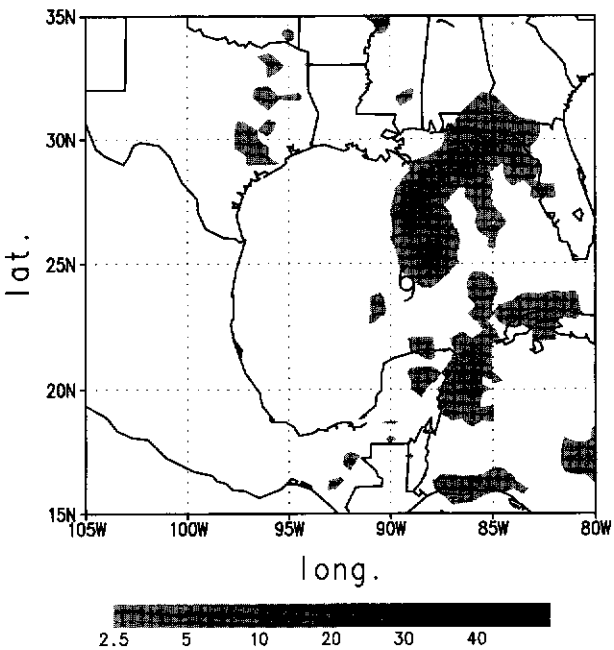

FIG. 4. Same as Fig. 3 except for 1200 UTC 9 September.

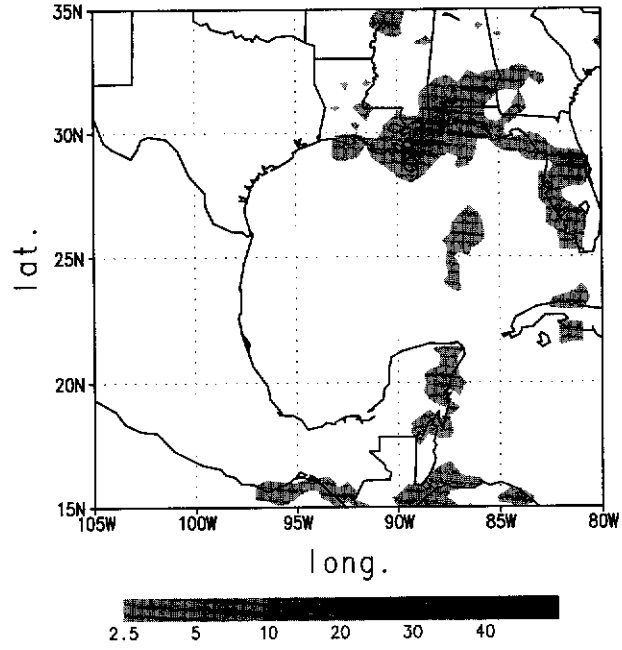

FIG. 5. Same as Fig. 3 except for 0000 UTC 10 September.

Mexico on 7 September. The frontal cloud band had previously been associated with a cold front, which entered the Gulf of Mexico from the northeast several days earlier. Florence was classified as a tropical depression with a maximum wind speed of 25 kt and a central pressure of 1000 mb at 0000 UTC 7 September. The depression quickly intensified into a tropical storm with a maximum wind speed of 40 kt and a central pressure of 998 mb at 1800 UTC 7 September. It moved eastward in the following 24 h and then turned northward on 8 September. The SSM/I rain rates at 0000 UTC 9 September (Fig. 3) show that the maxi-

TABLE 1. Best track record of Hurricane Florence (1988), obtained from the National Hurricane Center (NHC) in Miami, Florida.

Date	Time (UTC)	Position	Pressure (mb)	Wind ($m\ s^{-1}$)	Stage
7 Sep	0600	22.8°N, 92.0°W	1000	12.9	Tropical depression
	1200	22.8°N, 91.2°W	998	15.4	Tropical depression
	1800	22.7°N, 90.2°W	996	20.6	Tropical storm
8 Sep	0000	22.6°N, 89.6°W	993	23.1	Tropical storm
	0600	22.7°N, 89.8°W	990	23.1	Tropical storm
	1200	23.1°N, 89.7°W	990	23.1	Tropical storm
	1800	23.4°N, 89.5°W	992	23.1	Tropical storm
9 Sep	0000	24.2°N, 89.2°W	992	25.7	Tropical storm
	0600	25.0°N, 89.2°W	991	25.7	Tropical storm
	1200	26.1°N, 89.2°W	988	28.3	Tropical storm
	1800	27.4°N, 89.2°W	985	33.4	Hurricane
10 Sep	0000	28.7°N, 89.3°W	983	36.0	Hurricane
	0600	29.7°N, 89.7°W	988	30.9	Tropical storm
	1200	30.7°N, 90.7°W	998	15.4	Tropical depression
	1800	31.8°N, 91.5°W	1003	10.3	Tropical depression
11 Sep	0000	32.4°N, 92.3°W	1007	7.7	Tropical depression
	0600	32.7°N, 93.3°W	1009	7.7	Tropical depression
	1200	33.0°N, 94.5°W	1010	7.7	Tropical depression
9 Sep	2300	28.5°N, 89.3°W	982	36.0	Minimum pressure
10 Sep	0200	29.1°N, 89.3°W	984	36.0	Landfall

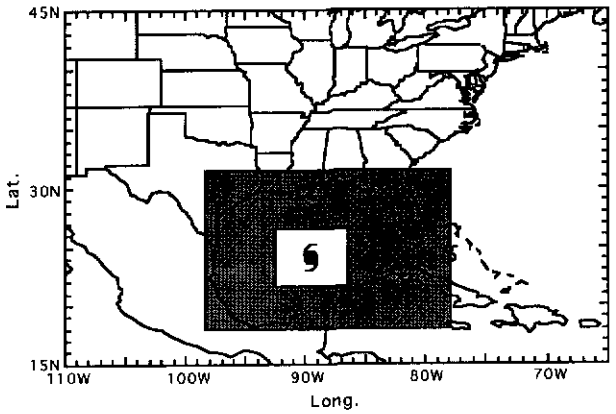

FIG. 6. Analysis domain for the nested three-pass objective analysis. Shaded area is for the first and second pass. Plain area inside the shaded area is for the third pass. The hurricane symbol depicts the location of Florence's center at 0000 UTC 9 September.

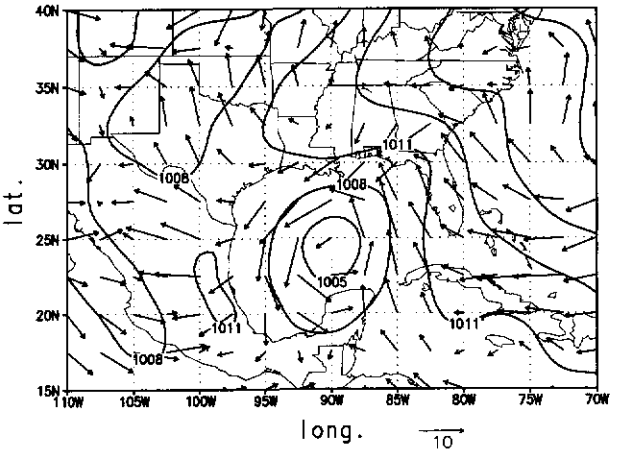

FIG. 7. Sea level pressures (mb) and 1000-mb winds (m s^{-1}) from the NMC/RAFS 2.5° analysis at 0000 UTC 9 September.

mum rain rates (~24 mm h^{-1}) associated with Florence were located south of the storm center. During the next 12 h from 0000 to 1200 UTC 9 September, the deep convection intensified rapidly. As shown in Fig. 4, the SSM/I rain rates indicate that a new convective cell located north of the low center with a maximum rain rate around 33 mm h^{-1} had developed during this 12-h period. This was confirmed by GOES infrared imagery (Rodgers et al. 1991). Florence continued to intensify and move northward on 9 September, and became a category-1 hurricane with a maximum wind speed of 65 kt and a central pressure of 985 mb at 1800 UTC 9 September. Figure 5 reveals the SSM/I rain rates at 0000 UTC 10 September. The heaviest precipitating region was north of the storm center near the coast of Louisiana with a maximum rain rate of about 18 mm h^{-1}. Florence still maintained a hurricane force at this time. Florence made landfall over southeastern Louisiana coast at 0200 UTC 10 September, and quickly weakened as it moved over the New Orleans area, before finally dissipating in eastern Texas (Lawrence and Gross 1989) on 11 September. The life span of Florence's circulation lasted only for about 4 days.

According to the best track data from the National Hurricane Center (NHC), Florence attained hurricane force for only 12 h, between 1200 UTC 9 September and 0600 UTC 10 September (Table 1). Estimated from the Air Force reconnaissance flight data, the highest sustained surface wind was 36 m s^{-1} and the lowest surface pressure 982 mb, occurring at 2300 UTC 9 September, just 3 h before landfall. Rainfall totals of up to 100 mm were observed along the path of the storm (Lawrence and Gross 1989). Florence caused the water level to rise from 1 to 2 m above normal along the southeast Louisiana and Mississippi coast just east of where the center moved ashore.

4. Regional analysis and forecast system

The research version of the NORAPS/NRL employed in this study includes a data assimilation system, a VMI, and a limited-area numerical model. The data assimilation includes two steps. The first step is a data preparation and quality control scheme and the second step is an objective analysis scheme. The data quality control consists of a "gross" check and a "buddy" check following DiMego (1988). Two different objective analysis schemes are available for the NRL model—a three-pass nested-grid Barnes scheme and a single-grid multivariate, successive correction objective scheme using the Bratseth method (Sashegyi et al. 1993). In this study, the three-pass nested-grid Barnes scheme was used. The vertical-mode initialization of NRL is described in Sashegyi and Madala (1993). This VMI scheme produces a balanced vertical motion

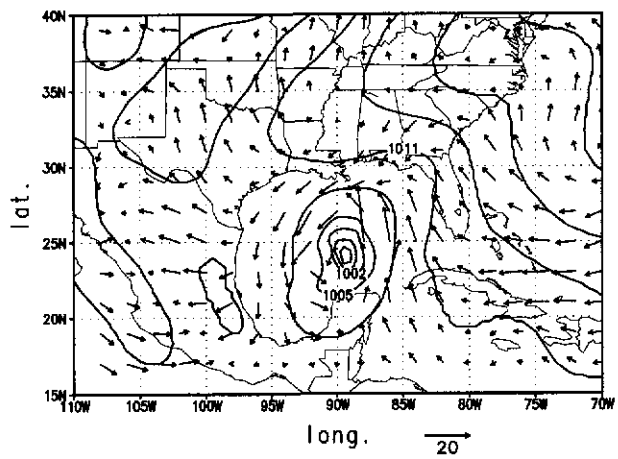

FIG. 8. Sea level pressures (mb) and 1000-mb winds (m s^{-1}) from the ODW enhanced analysis at 0000 UTC 9 September.

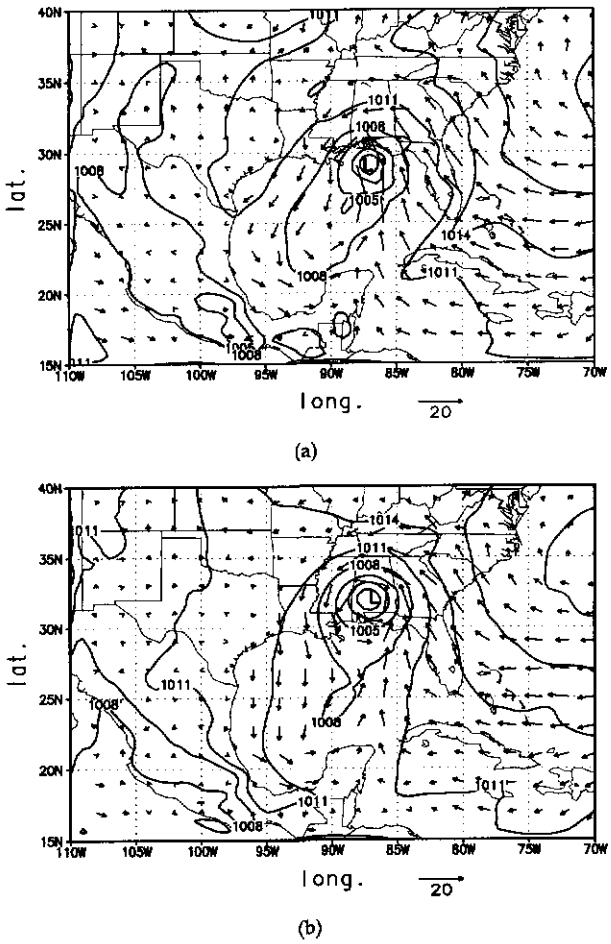

FIG. 9. Same as Fig. 7 except for the NMC/RAFS 2.5° analysis at (a) 1200 UTC 9 September and (b) 0000 UTC 10 September.

field and induces smaller changes to the initial mass and wind fields as compared to static initialization schemes.

The limited-area prognostic model is a three-dimensional, hydrostatic, primitive equation model incorporating a split-explicit time integration scheme (Madala 1981). Details of the model are described in Madala et al. (1987), Chang et al. (1989), and Holt et al. (1990). The version of the model used in this study has 23 layers in the vertical. A terrain following $\sigma(=P/P_s)$ vertical coordinate and time-dependent lateral boundary conditions are utilized, where P is the pressure and P_s the surface pressure. Topography used in this model is derived from the United States Navy global 10′ elevation data. The model domain covers 15°–45°N, 110°–65°W including most of the continental United States and all the Gulf of Mexico, with horizontal resolutions of $1/2°$ and $1/3°$ in longitude and latitude directions, respectively.

The sea surface temperature analysis is obtained from the multichannel sea surface temperature (MCSST) data derived from AVHRR (Advanced Very High Resolution Radiometer) imagery. This MCSST product is a weekly composite at a horizontal resolution of approximately 18 km. The model uses a modified Kuo scheme for cumulus convection (Kuo 1965; Anthes 1977). The large-scale precipitation occurs when there is a supersaturated layer in the model. The excess moisture is condensed out isobarically with the released latent heat warming the air, leaving the layer saturated. Model physics also includes horizontal diffusion and dry convection adjustment.

5. Assimilation of the ODW data

The ODW data were used to enhance the NMC/RAFS 2.5° analyses at 0000 UTC 9 September. In a previous treatment of the ODW data for Florence, Kaplan and Franklin (1991) used a nested objected analysis scheme (Ooyama 1987), which employs a two-dimensional, least squares fitting algorithm with a derivative

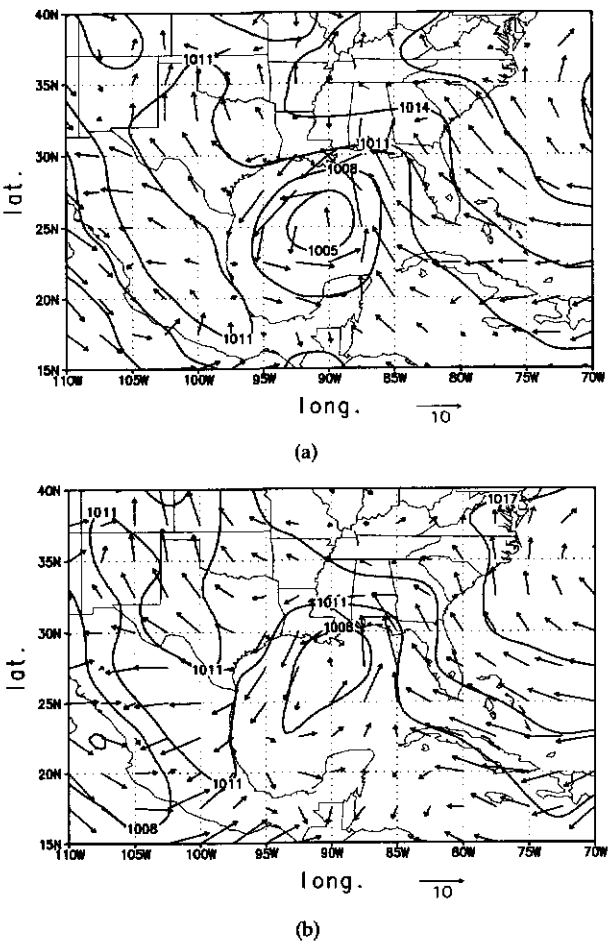

FIG. 10. Sea level pressures (mb) and 1000-mb winds (m s^{-1}) from the control experiment at (a) 12 h and (b) 24 h, valid at 1200 UTC 9 September and 0000 UTC 10 September, respectively.

TABLE 2. Minimum SLP (mb), maximum wind speed (m s^{-1}), and location of storm center from the best track record, the control experiment, and experiment ODW.

	0 h	6 h	12 h	18 h	24 h
			Minimum sea level pressure (mb)		
Best track record	992	991	988	985	983
Control	1006	1003	996	995	997
ODW	1005	1001	997	988	987
			Maximum surface wind speed (m s^{-1})		
Best track record	25.7	25.7	28.3	33.4	36.0
Control	14.1	23.7	33.6	28.6	22.2
ODW	28.4	24.4	30.4	35.8	38.8
			Location of storm center		
Best track record	24.2°N, 89.2°W	25.2°N, 89.2°W	26.1°N, 89.2°W	27.4°N, 89.2°W	28.7°N, 89.3°W
Control	24.9°N, 89.9°W	27.3°N, 87.1°W	29.1°N, 87.1°W	30.7°N, 86.8°W	32.1°N, 86.7°W
ODW	24.3°N, 89.4°W	25.6°N, 88.6°W	27.1°N, 88.8°W	28.5°N, 89.1°W	29.6°N, 89.3°W

constraint term, to analyze the ODW data. The derivative constraint term functions as a spatial low-pass filter on the analyzed field. In the present study, a three-pass nested-grid Barnes scheme was used. A time domain of 6 h from 2100 UTC 8 September to 0300 UTC 9 September was imposed to filter out the ODW data outside this time domain. The choice of a 6-h time domain centered at 0000 UTC 9 September was simply based on a 3-h data cutoff time commonly used in many operation forecasting centers.

The NMC/RAFS 2.5° analyses were bicubically interpolated to the model's grid as shown in Fig. 6, and used as the first guess. The first guess data were then bilinearly interpolated to the ODW data locations. The three-pass nested-grid Barnes scheme was employed to analyze the corrections that resulted from subtracting the interpolated first guess data from the ODW data. The analyzed corrections were then added back to the first guess at each grid point. The first two passes of the Barnes scheme were done in the shaded area including the plain area inside the shaded area, while the third pass was done only in the plain area (Fig. 6) using the analyzed results from the first two passes as the background data. The horizontal resolution was 1/2° in the first two passes and 1/6° in the third pass. The selection of the two resolutions for the three passes in the objective analysis was to match the varying ODW data resolutions over the Gulf of Mexico area (Fig. 1). The details and results of the ODW enhanced analyses for Hurricane Florence (1988) were documented in Shi et al. (1991) and Shi (1993). Figures 7 and 8 show the sea level pressures and 1000-mb isotaches from the NMC/RAFS 2.5° and the ODW enhanced analyses at 0000 UTC 9 September, respectively. It is apparent that the ODW enhanced analyses provide a more realistic depiction of Florence. Both the NMC/RAFS 2.5° and the ODW enhanced analyses were initialized by the VMI and used as the initial data for the model integration of the various numerical experiments.

6. Assimilation of the SSM/I rain rates

As mentioned earlier, a modified Kuo scheme is used in the numerical model for cumulus convection. Following the discussion in Chang and Holt (1994), the convective latent heating at a grid point in the model with the modified Kuo convective scheme is

$$\frac{\delta T}{\delta t} = \frac{bgLM_t(T_c - T)}{C_p P_s \int_\sigma (T_c - T)d\sigma}, \quad \text{if} \quad M_t > 0, \quad (1)$$

where b is a partitioning parameter set equal to the vertical mean relative humidity; T_c, the cloud temperature; L, the specific latent heat; C_p, the specific heat at constant pressure of air; and P_s, the surface pressure. Here, M_t is the total moisture convergence defined as

$$M_t = \frac{P_s}{g}\int_\sigma -\nabla\cdot \mathbf{V}qd\sigma, \quad (2)$$

where q is the specific humidity. The rain rate $\delta R/\delta t$ (cm s^{-1}) in the model, which is related to the vertically integrated heating rate, is then defined at each grid point as

$$\frac{\delta R}{\delta t} = \frac{P_s C_p}{g\rho_w L}\int_\sigma \frac{\delta T}{\delta t}d\sigma, \quad (3)$$

where ρ_w is the density of liquid water. In the assimilation experiments presented here, the left-hand side of (3) was replaced by the SSM/I-retrieved rain rates in the area inside the SSM/I swath within the assimilation windows. The assimilation window was between 0 and 3 h of the integration for the SSM/I overpass at 0000

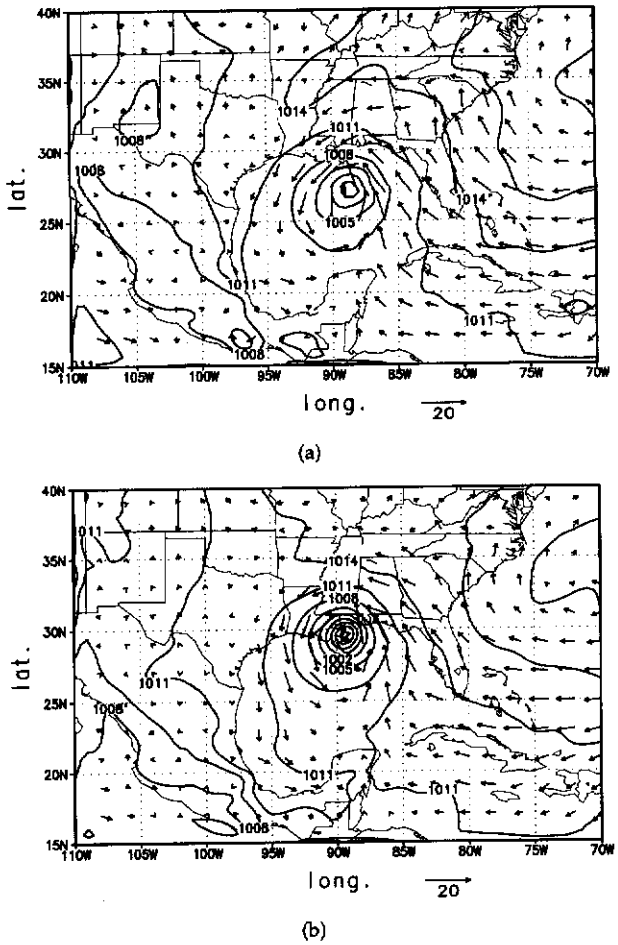

FIG. 11. Same as Fig. 10 except for experiment ODW.

UTC 9 September and 9–15 h for the SSM/I overpass at 1200 UTC 9 September. The rain rates outside the SSM/I swath were not changed.

7. Simulation results

To assess the impact of the ODW and the SSM/I rain rate data on the numerical simulation of Hurricane Florence (1988), model integrations using different initial data were conducted. All the model runs were started at 0000 UTC 9 September and integrated for 48 h. The first numerical simulation (the control experiment) used the NMC/RAFS 2.5° analyses at 0000 UTC 9 September as the initial condition, while the second experiment (experiment ODW) used the ODW enhanced analyses as the initial condition. The third (experiment control + SSMI) and the fourth (experiment ODW + SSMI) experiments were the same as the first and the second experiments, respectively, except that the SSM/I rain rates were assimilated into the model during the integration by using the approach described in the previous section. The last two experiments were designed to study the impact of the SSM/I rain rates on the numerical simulation.

a. Intensity

Figure 10 shows the sea level pressures (SLPs) and the 1000-mb wind vectors at 12 and 24 h from the control experiment valid at 1200 UTC 9 September and 0000 UTC 10 September. For comparison, Fig. 9 shows the NMC/RAFS 2.5° analyses at 1200 UTC 9 September and 0000 10 September. The minimum SLPs of the control experiment were 996 and 997 mb at 12 and 24 h, respectively. Compared with the best track record shown in Table 1 and the NMC/RAFS 2.5° analyses (Fig. 9), the simulated storm in the control experiment moved northward faster than the best track record and was much weaker than the best track record by an average of greater than 10 mb, but stronger than the storm depicted in the NMC/RAFS 2.5° analyses. The maximum surface wind speeds in the control experiment were 33.6 and 22.2 m s^{-1} at 12 and 24 h, respectively (Table 2). The simulated storm at 24 h in the control experiment had a min-

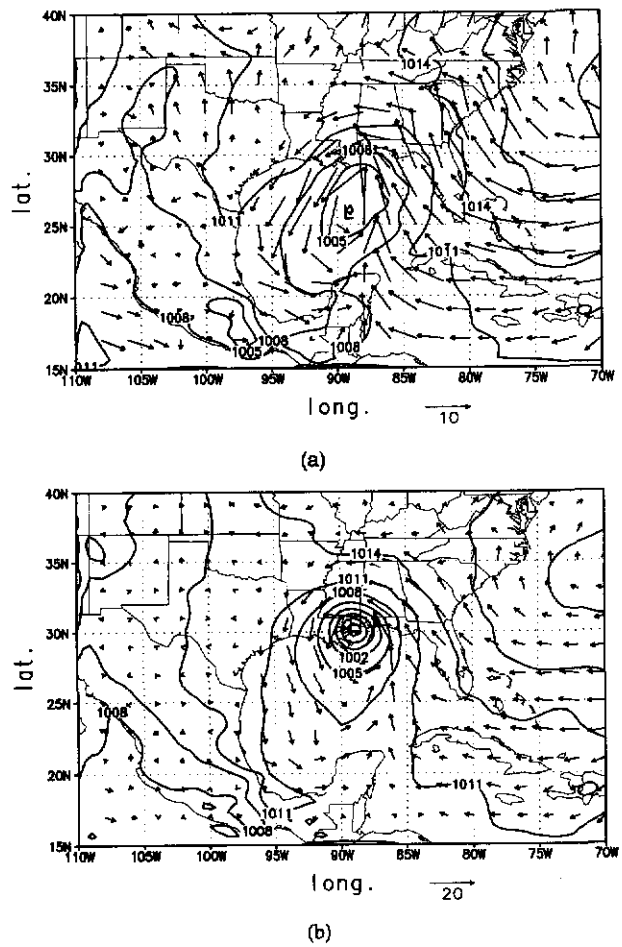

FIG. 12. Same as Fig. 10 except for experiment control + SSMI.

TABLE 3. Minimum SLP (mb), maximum wind speed (m s^{-1}), and location of storm center from the best track record and experiments control + SSMI and ODW + SSMI.

	0 h	6 h	12 h	18 h	24 h
			Minimum sea level pressure (mb)		
Best track record	992	991	988	985	983
Control + SSMI	1006	1004	1002	999	992
ODW + SSMI	1005	1003	999	992	985
			Maximum surface wind speed (m s^{-1})		
Best track record	25.7	25.7	28.3	33.4	36.0
Control + SSMI	14.1	20.3	23.1	29.3	32.3
ODW + SSMI	28.4	20.0	24.2	34.5	38.3
			Location of storm center		
Best track record	24.2°N, 89.2°W	25.2°N, 89.2°W	26.1°N, 89.2°W	27.4°N, 89.2°W	28.7°N, 89.3°W
Control + SSMI	24.9°N, 89.9°W	25.3°N, 89.0°W	25.9°N, 89.1°W	27.4°N, 88.5°W	30.6°N, 88.9°W
ODW + SSMI	24.3°N, 89.4°W	25.5°N, 89.1°W	26.5°N, 89.4°W	27.5°N, 89.2°W	29.0°N, 89.6°W

imum SLP 14 mb higher and a maximum surface wind speed 13.8 m s^{-1} lower than what the best track indicated, a rather poor intensity forecast.

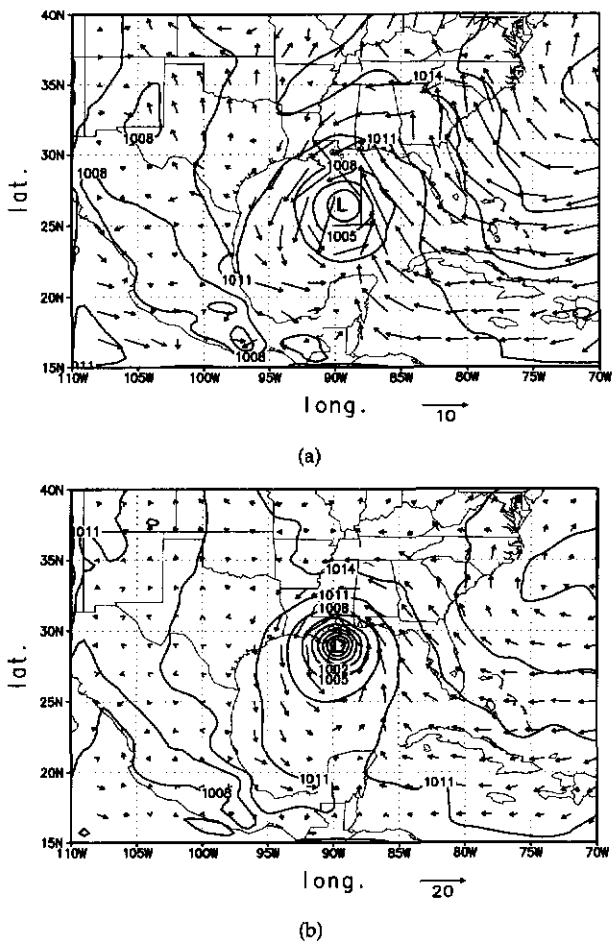

FIG. 13. Same as Fig. 10 except for experiment ODW + SSMI.

Experiment ODW was initialized on the ODW enhanced analysis, with the SLPs and the 1000-mb wind vectors at 12 and 24 h shown in Fig. 11. The minimum SLPs of the storm in experiment ODW were 997 and 987 mb at 12 and 24 h, respectively. The maximum surface wind speeds of the simulated storm in experiment ODW were 30.4 and 38.8 m s^{-1} at 12 and 24 h, respectively (Table 2). It is apparent that the intensity of the simulated storm in experiment ODW was stronger in comparison to the control experiment (Fig. 10) and in the NMC/RAFS 2.5° analyses (Fig. 9). The minimum SLP and maximum surface wind speed of experiment ODW at 24 h valid at 0000 UTC 10 September was about 4 mb weaker and 2.8 m s^{-1} stronger than the best track verification. The assimilation of the ODW data into the initial data has thus improved the intensity forecast relative to the control experiment by 10 mb for the minimum SLP and 11 m s^{-1} for the maximum surface wind speed at 24 h.

Figure 12 shows the SLPs and the 1000-mb wind vectors in experiment control + SSMI at 12 and 24 h. The minimum SLPs of the simulated storm in experiment control + SSMI were 1002 and 992 mb at 12 and 24 h, respectively (Table 3). The maximum surface wind speed of experiment control + SSMI at 12 and 24 h were 23.1 and 32.3 m s^{-1}, respectively (Table 3). Compared to the control experiment, the 24-h minimum SLP and maximum wind speed forecast in experiment control + SSMI valid at 0000 UTC September 10 were superior by 5 mb and 10.1 m s^{-1}, respectively, relative to the best track record.

Figure 13 shows the SLPs and the 1000-mb wind vectors in experiment ODW + SSMI at 12 and 24 h. The minimum SLPs at 12 and 24 h were 999 and 985 mb, respectively, and the corresponding maximum wind speeds were 24.2 and 38.3 m s^{-1}, respectively (Table 3). Comparing the results from experiment ODW and ODW + SSMI (Tables 2 and 3) with the

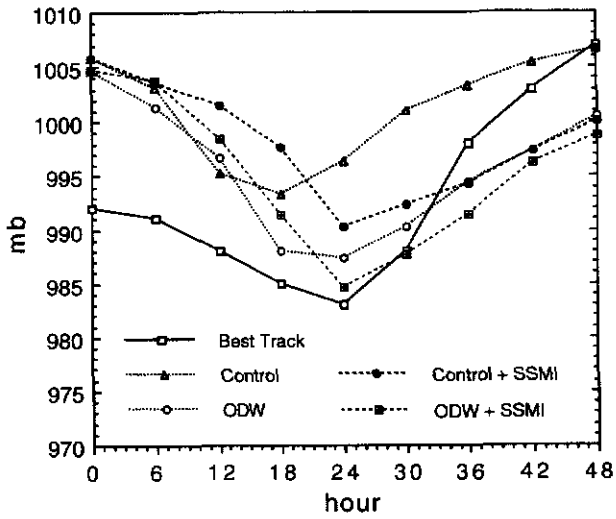

FIG. 14. Evolution of minimum sea level pressure of Florence with time in the best track record, the control experiment, and experiments control + SSMI, ODW, and ODW + SSMI.

best track record, the assimilation of the SSM/I rain rates in experiment ODW + SSMI has improved the 24-h prediction of the minimum SLP by 2 mb (down from 987 mb in experiment ODW to 985 mb), and the maximum wind speed by 0.5 m s^{-1}. Although the assimilation of the SSM/I rain rates did not improve much over experiment ODW, it provided the best 24-h intensity forecast among all four model simulations. Figure 14 shows the evolution of the minimum SLP with time from the best track and all four experiments. It is obvious that experiment ODW + SSMI produced the best minimum SLP forecast at 24 h and the control experiment produced the worst. This study shows that both the ODW data and SSM/I rain rates made positive impacts on the numerical prediction of the intensity of Hurricane Florence (1988) at 12–30 h. At 48 h, however, the impact of the assimilation of both the ODW data and SSM/I rain rates diminished enough that the difference is not discernible. This also suggests that an update cycle with more frequent data assimilations is important for accurate numerical predictions.

b. Track

The 48-h tracks from the best track and all four experiments (Fig. 15) show that the simulated storm in the control experiment moved faster than the observation. The simulated storm in the control experiment

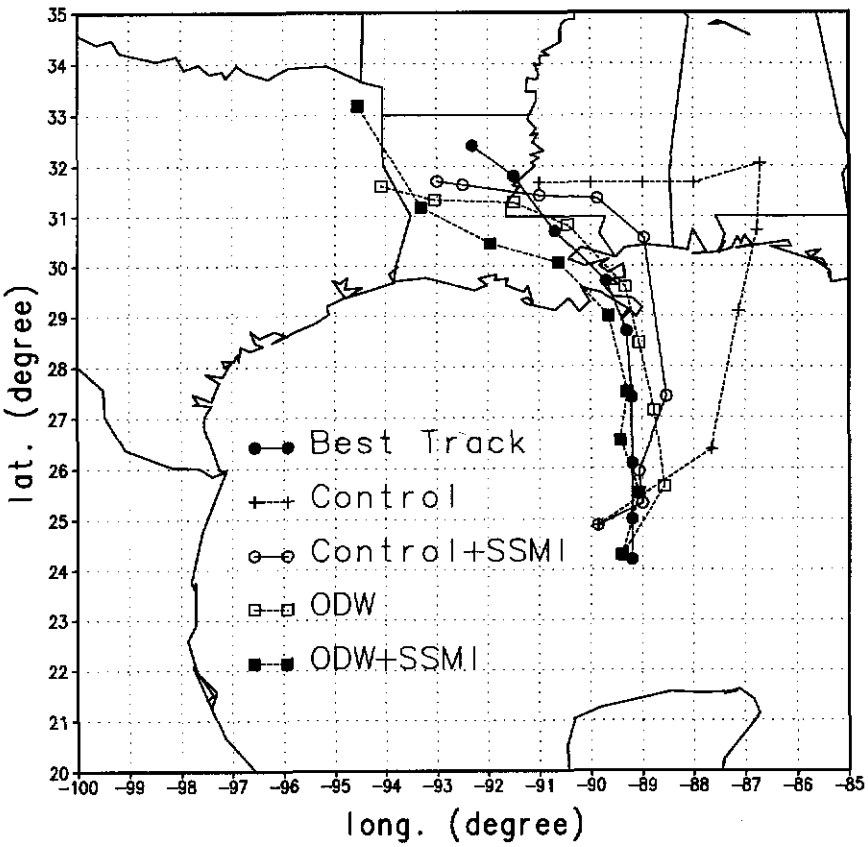

FIG. 15. Tracks of Florence in the best track record, control experiment, and experiments ODW, control + SSMI, and ODW + SSMI.

made landfall at 1700 UTC 9 September 1988, about 9 h (Table 4) earlier than the landfall time in the best track. The forecast landfall location was about 294 km northeast of the location in the best track. The track forecast in the control experiment is poor, mainly because the NMC/RAFS 2.5° analysis failed to resolve the storm properly and to provide the accurate environmental steering force. As listed in Table 4, it shows that the forecast storm in experiment control + SSMI made landfall only 2 h earlier than the landfall time in the best track and at a location about 169 km north of the location in the best track. This is an improvement of about 7 h in landfall time and 43% in landfall location over the control experiment. In experiment ODW, the landfall time was 4 h earlier than the actual landfall and the landfall location was about 15 km southeast of the actual landfall location. In experiment ODW + SSMI, the landfall time was exactly predicted and the landfall location was about 69 km northwest of the actual landfall location. While experiment ODW predicted the best landfall location, experiment ODW + SSMI produced the exact landfall time.

Among the four predicted tracks in Fig. 15, it is apparent that experiment ODW + SSMI produced the best forecast of the track of Hurricane Florence (1988). Because the initial storm location in the ODW enhanced analysis was better than in the NMC/RAFS 2.5° analysis, and the better wind analysis provided by the ODW data resulted in more accurate environmental steering, the predicted tracks in experiments ODW and ODW + SSMI were better than those in the control experiment and experiment control + SSMI. Figure 15 also shows that the storms in experiments control + SSMI and ODW + SSMI moved slower than those in the control experiment and experiment ODW. It is believed that the more accurate latent heating furnished by the SSM/I data effectively slowed down the movement of the predicted storms. It leaves no doubt that both ODW data and SSM/I rain rates have positive impact on the track forecast of Hurricane Florence (1988). However, the ODW data are relatively rare observations that require a nonordinary effort to collect them, while the SSM/I supplies near-real time and up to six observations per day depending on the latitude. The track improvement shown in experiment Control + SSMI is significant. The predicted storm tracks in the second 24 h were less accurate than those in the first 24 h. This again underscores that an update cycle with more frequent data assimilations is needed.

c. *Precipitation pattern*

The simulated rain rates at 24 h from the different experiments were compared to the verifying SSM/I rain rates at 0000 UTC 10 September 1988 (Fig. 5) to verify the model simulations and to investigate the impact of assimilations. At 24 h valid at 0000 UTC September 10, the heaviest rain rates (>20 mm h^{-1}) in the control experiment (Fig. 16) were located far inland in Georgia with the heavy rain-rate region stretching southward into the Gulf of Mexico. The heaviest SSM/I-observed rain rates (>15 mm h^{-1}) were located near New Orleans (see Fig. 5) at 0000 UTC September 10. It is apparent that the control experiment misplaced the precipitation of Florence mainly because of the poor location forecast. The heaviest forecasted rainfall (>40 mm h^{-1}) in experiment ODW at 24 h was located just off the coast of Mississippi in a northeast–southwest oriented rain band (see Fig. 17). The heavy rain-rate region started at the border of Alabama and Georgia and extended southwestward into the Gulf of Mexico off the Louisiana coast. The rainfall pattern in experiment ODW had the same northeast to southwest orientation as in the SSM/I rain rates (Fig. 5), except the SSM/I retrieval had a much lighter maximum rain rate (>15 mm h^{-1}). Previous studies have shown that the SSM/I rain rates are a good analysis tool for hurricanes (Rodgers et al. 1991; Alliss et al. 1992, 1993) and midlatitude marine cyclone studies (Chang et al. 1993). As pointed out in (Chang and Holt 1994), SSM/I rain-rate retrieval is invaluable in identifying the precipitation patterns in spite of the uncertainties in rain-rate estimates. This study has shown that the forecast rain patterns at 24 h in experiment ODW agreed well with the verifying SSM/I rain patterns.

With the assimilation of the SSM/I rain rates, the simulated rain rates in experiment control + SSMI (Fig. 18) at 24 h showed that the heaviest rain rates

TABLE 4. Landfall times and locations from the best track record, the control experiment, and experiments control + SSMI, ODW, and ODW + SSMI. The landfall locations relative to the location shown in the best track record are also listed.

		Landfall location	
	Landfall time	Lat./Long.	Relative location to best track
Best track record	0200 UTC 10 Sep 93	29.1°N, 89.3°W	
Control experiment	1700 UTC 9 Sep 93	30.5°N, 86.7°W	294 km northeast
Exp. control + SSMI	0000 UTC 10 Sep 93	30.6°N, 88.9°W	169 km north
Exp. ODW	2200 UTC 9 Sep 93	29.0°N, 89.2°W	15 km southeast
Exp. ODW + SSMI	0200 UTC 10 Sep 93	29.2°N, 89.9°W	69 km northwest

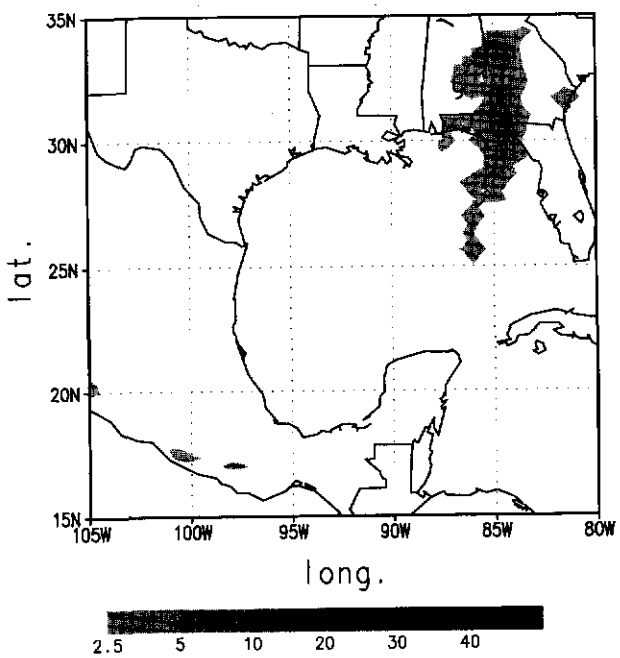

FIG. 16. Predicted rain rate (mm h^{-1}) of the control experiment at 24 h valid at 0000 UTC 10 September. The hurricane symbol depicts the location of the predicted storm center.

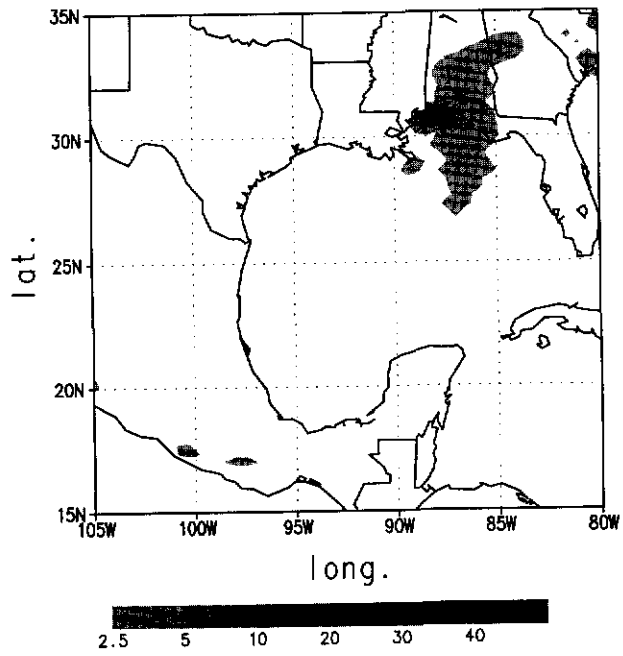

FIG. 18. Same as Fig. 16 except for experiment control + SSMI.

(>40 mm h^{-1}) were located at southern Alabama and Mississippi near the coast and extended from central Alabama into the Gulf of Mexico. Comparison of Figs. 18 and 5 reveals that the simulated rain rates did not agree well with the verifying SSM/I rain rates in pattern and intensity, but had improved on the poorly forecasted rain rates in the control experiment. The simulated rain rates in experiment ODW + SSMI at 24 h are shown in Fig. 19. The heaviest rain rates (>30 mm h^{-1}) were located just east of New Orleans and north of the Mississippi River delta. The pattern of the forecasted rain rates in this experiment was similar to the one in experiment ODW and the verifying SSM/I rain rates. However, the maximum intensity of the simulated rain rates was weaker than the maximum intensity (>40 mm h^{-1}) in experiment ODW.

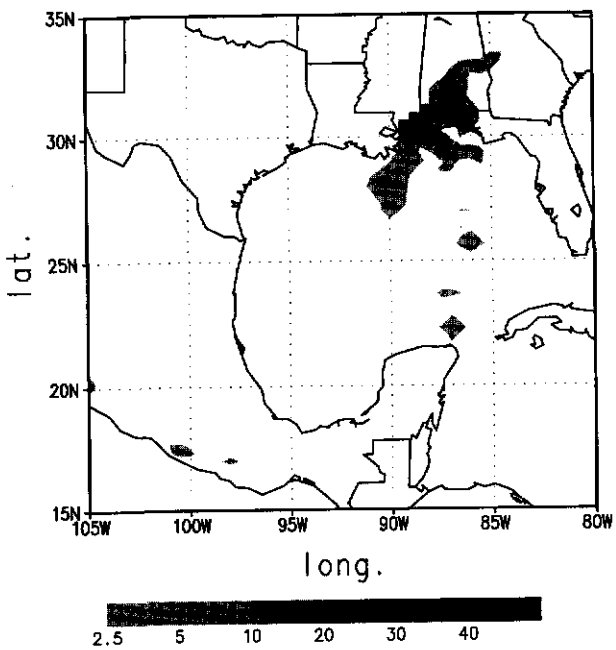

FIG. 17. Same as Fig. 16 except for experiment ODW.

8. Summary and discussion

Four numerical simulations were performed to assess the impact of ODW data and SSM/I rain rates on numerical forecasts of Hurricane Florence (1988). A nested three-pass Barnes scheme objective analysis was used to enhance the NMC/RAFS 2.5° analysis because of the relative high resolution of the ODW data near the center of Florence. The NMC/RAFS 2.5° analysis and the ODW enhanced analysis were then used as the initial conditions for the numerical prediction experiments. We found that the forecast error of the intensity was reduced from 14 to 4 mb with the assimilation of the ODW data. It is also clear from Table 4 that the ODW data reduced the forecast error of the landfall time in the control experiment by 5 h (down from 9 to 4 h), and the landfall location error by 95% (down from 294 to 15 km). The impact of the ODW data was

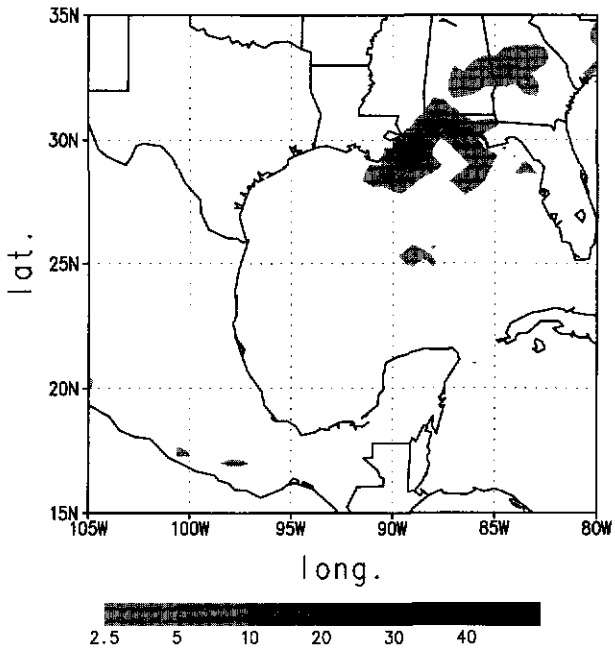

FIG. 19. Same as Fig. 16 except for experiment ODW + SSMI.

more pronounced in the first 24 h of the integration (Figs. 14 and 15) and gradually decreased beyond 24 h. This result is in agreement with Franklin and DeMaria (1992), in which a barotropic, nested, spectral hurricane track forecasting model was used to determine the impact of the ODW data. The advantage of using a three-dimensional primitive equation model with the inclusion of baroclinic and physical processes, as in this study, is that the model can simulate the hurricane structure in more detail (DeMaria et al. 1992). However, a major limitation of the ODW observations is that they do not provide information above 400 mb because of the altitude limitations of the NOAA WP-3D. While satellite-derived winds can provide some upper-level information (Velden et al. 1992), detailed observations of the three-dimensional structure of the upper levels of tropical cyclones are extremely scarce. Dropsonde data collected from 200 mb to the surface by the recent TCM-90 experiment (Elsberry and Abbey 1991) may be proven to be very useful in depicting the upper-level structure of tropical cyclones (Merrill and Velden 1996).

The rainfall rates retrieved from the SSM/I data at 0000 UTC and 1200 UTC 9 September 1988 were assimilated into the NRL limited-area model initialized with the NMC/RAFS 2.5° analysis (experiment control + SSMI) and the ODW enhanced analysis (experiment ODW + SSMI). Results indicate that the assimilation of the SSM/I rain rates (experiment control + SSMI) reduced the 24-h forecast errors in the landfall location in the control experiment by about 43% (down from 294 to 169 km), and the landfall time by 5 h (down from 9 to 4 h). At mean time, the 24-h minimum SLP and maximum surface wind speed forecasts were also improved by 5 mb and 10.1 m s^{-1}, respectively. This study suggests that the assimilation of SSM/I rain rates can improve the track and intensity forecasts of tropical cyclones, especially when the ODW data are not available to the operational analysis. The benefit of the assimilation of SSM/I rain rates was limited when the simultaneous ODW data had already been assimilated into the initial condition, and vice versa. The landfall time error was reduced from 4 to 0 h, and there was an improvement on the predicted storm track when the SSM/I rain rates were assimilated. The intensity forecast was also improved with the 24-h minimum SLP forecast error reduced by 2 mb. There is no question that the combination of the ODW data and SSM/I rain rates provided the best simulation at 24 h in this study. Results from this study agree with the assessment of Chang and Holt (1994) regarding the positive impact of assimilating SSM/I rain rates on the numerical predictions. This study suggests that operational forecasts can benefit from the assimilation of ODW and SSM/I data into numerical models for the prediction of the intensity and track of tropical cyclones. The increase of the track forecast accuracy will allow forecasters to reduce the overwarned area in the warning process and result in reducing the preparation costs incurred by the public in coastal areas (Sheet 1990; Franklin et al. 1991). In any case study, the question arises whether or not the behavior shown is relevant to a large group of tropical cyclones. More studies need to be performed to further explore the value of both ODW and SSM/I data for the numerical forecast of tropical cyclones, especially when the ODW data collected from 200 mb to the surface become available from the AOML/HRD. The upper-tropospheric influence to the intensity and track change of tropical cyclones has long been recognized.

Acknowledgments. The authors wish to thank Dr. Keith Sashegyi of NRL for providing the help on NRL's data analysis system, Mr. Glenn Sandlin of NRL for providing the SSM/I imagery data, and Mr. Randy Alliss of North Carolina State University for processing the SSM/I imagery data for us. We also want to extend our appreciation to Dr. James Franklin of the AOML/HRD for providing the ODW data to the research community. The research was supported by the NRL basic research program.

REFERENCES

Alliss, R. J., S. Raman, and S. Chang, 1992: Special Sensor Microwave/Imager (SSM/I) observation of Hurricane Hugo (1989). *Mon. Wea. Rev.*, **120,** 2723–2737.

——, G. D. Sandlin, S. W. Chang, and S. Raman, 1993: Application of SSM/I data in the analysis of Hurricane Florence (1988). *J. Appl. Meteor.*, **32,** 1581–1591.

Anthes, R. A., 1977: A cumulus parameterization scheme utilizing a one-dimensional cloud model. *Mon. Wea. Rev.*, **105,** 270–286.

——, 1982: *Tropical Cyclones: Their Evolution, Structure and Effects.* Vol. 19, American Meteorological Society, 208 pp.

Bender, M. A., R. J. Ross, Y. Kurihara, and R. E. Tuleya, 1991: Improvements in tropical cyclone track and intensity forecasts using a bogus vortex. Preprints, *19th Conf. on Hurricanes and Tropical Meteorology,* Miami, FL, Amer. Meteor. Soc., 324–325.

Chang, S. W., and T. R. Holt, 1994: Impact of assimilating SSM/I rainfall rates on numerical prediction of winter cyclones. *Mon. Wea. Rev.,* **122,** 151–164.

——, K. Brehme, R. V. Madala, and K. D. Sashegyi, 1989: A numerical study of the east coast snowstorm of 10–12 February 1983. *Mon. Wea. Rev.,* **117,** 1768–1778.

——, R. J. Alliss, S. Raman, and J. J. Shi, 1993: SSM/I observations of ERICA/IOP 4 marine cyclone: A comparison with in situ observations and model simulation. *Mon. Wea. Rev.,* **121,** 2452–2464.

Davidson, N. E., and K. Puri, 1992: Tropical prediction using dynamic nudging, satellite-defined convective heat sources, and a cyclone bogus. *Mon. Wea. Rev.,* **120,** 2501–2522.

DeMaria, M., S. D. Aberson, and K. V. Ooyama, 1992: A nested spectral model for hurricane track forecasting. *Mon. Wea. Rev.,* **120,** 1628–1643.

DiMego, G., 1988: The National Meteorological Center regional analysis system. *Mon. Wea. Rev.,* **116,** 977–1000.

Elsberry, R. L., and R. F. Abbey Jr., 1991: Overview of the tropical cyclone motion (TCM-90) field experiment. Preprints, *19th Conf. on Hurricanes and Tropical Meteorology,* Miami, FL, Amer. Meteor. Soc., 1–6.

Ferriday, J. G., and S. K. Avery, 1994: Passive microwave remote sensing of rainfall with SSM/I: Algorithm development and implementation. *J. Appl. Meteor.,* **33,** 1587–1596.

Fiorino, M., and T. T. Warner, 1981: Incorporating surface winds and rainfall rates into the initialization of a mesoscale hurricane model. *Mon. Wea. Rev.,* **109,** 1914–1929.

Franklin, J. L., and M. DeMaria, 1992: The impact of Omega dropwindsonde observations on barotropic hurricane track forecasts. *Mon. Wea. Rev.,* **120,** 381–391.

——, ——, and C. S. Velden, 1991: The impact of Omega Dropwindsonde and satellite data on hurricane track forecasts. Preprints, *19th Conf. on Hurricanes and Tropical Meteorology,* Miami, FL, Amer. Meteor. Soc., 87–92.

——, S. J. Lord, S. E. Feuer, and F. D. Marks Jr., 1993: The kinematic structure of Hurricane Gloria (1985) determined from nested analyses dropwindsonde and Doppler radar data. *Mon. Wea. Rev.,* **121,** 2433–2451.

Goerss, J., and P. Phoebus, 1992: The Navy's operational atmospheric analysis. *Wea. Forecasting,* **7,** 232–249.

Hollinger, J. P., 1989: DMSP Special Sensor Microwave/Imager calibration. Final Rep. Vol. I, 176 pp. [Available from the author at Naval Research Laboratory, Washington, DC 20375.]

——, 1991: DMSP Special Sensor Microwave/Imager calibration. Final Rep. Vol. II, 277 pp. [Available from the author at Naval Research Laboratory, Washington, DC 20375.]

Holt, T., S. W. Chang, and S. Raman, 1990: A numerical study of the coastal cyclogenesis in GALE IOP 2: Sensitivity to PBL parameterizations. *Mon. Wea. Rev.,* **118,** 234–257.

Kaplan, J., and J. L. Franklin, 1991: The relationship between the motion of tropical storm Florence (1988) and its environmental flow. Preprints, *19th Conf. on Hurricanes and Tropical Meteorology,* Miami, FL, Amer. Meteor. Soc., 93–97.

Kuo, H. L., 1965: On formation and intensification of tropical cyclones through latent heat release by cumulus convection. *J. Atmos. Sci.,* **22,** 40–63.

Lawrence, M. B., and J. M. Gross, 1989: Atlantic hurricane season of 1988. *Mon. Wea. Rev.,* **117,** 2248–2259.

Lord, S. J., 1991: A bogusing system for vortex circulations in the National Meteorological Center global forecast model. Preprints, *19th Conf. on Hurricanes and Tropical Meteorology,* Miami, FL, Amer. Meteor. Soc., 328–330.

Madala, R. V., 1981: Efficient time integration schemes for atmospheric and ocean models. *Finite Difference Techniques for Vectorized Fluid Dynamic Calculations,* Springer-Verlag, 56–74.

——, S. W. Chang, U. C. Mohanty, S. C. Madan, R. K. Paliwal, V. B. Sarin, T. Holt, and S. Raman, 1987: Description of the naval research laboratory limited-area dynamical Weather prediction model. NRL Tech. Rep. 5992, 131 pp. [NTIS A182780.]

Merrill, R. T., and C. S. Velden, 1996: A three-dimensional analysis of the outflow layer of Supertyphoon Flo (1990). *Mon. Wea. Rev.,* **124,** 47–63.

Molinari, J., 1982: Numerical hurricane prediction using remotely-sensed rainfall rates. *Mon. Wea. Rev.,* **110,** 553–571.

Neumann, C. J., 1981: Trends in forecasting the tracks of Atlantic tropical cyclones. *Bull. Amer. Meteor. Soc.,* **62,** 1473–1485.

Ooyama, K. V., 1987: Scale controlled objective analysis. *Mon. Wea. Rev.,* **115,** 2479–2506.

Rao, G. V., and P. D. MacArthur, 1994: The SSM/I estimated rainfall amounts of tropical cyclones and their potential in predicting the cyclone intensity changes. *Mon. Wea. Rev.,* **122,** 1568–1574.

Rodgers, E. B., S. W. Chang, J. Stout, J. Steranka, and J. J. Shi, 1991: Satellite observations of variations in tropical cyclone convection caused by upper-tropospheric troughs. *J. Appl. Meteor.,* **30,** 1163–1184.

——, ——, and H. F. Pierce, 1994: A satellite observational and numerical study of precipitation characteristics in western North Atlantic tropical cyclones. *J. Appl. Meteor.,* **33,** 129–139.

Sashegyi, K. D., and R. V. Madala, 1993: Application of vertical-mode initialization to a limited-area model in flux form. *Mon. Wea. Rev.,* **121,** 207–220.

——, D. E. Harms, R. V. Madala, and S. Raman, 1993: Application of Bratseth scheme for the analysis of GALE data using a mesoscale model. *Mon. Wea. Rev.,* **121,** 2331–2350.

Sheet, R. C., 1990: The National Hurricane Center—Past, present, and future. *Wea. Forecasting,* **5,** 185–232.

Shi, J. J., 1993: Numerical investigation of the interaction between Hurricane Florence (1988) and its upper-level environment. Ph.D. dissertation, North Carolina State University at Raleigh, 206 pp.

——, S. W. Chang, K. D. Sashegyi, and S. Raman, 1991: Enhancement of objective analysis of Hurricane Florence (1988) with dropsonde data. Preprints, *19th Conf. on Hurricanes and Tropical Meteorology,* Miami, FL, Amer. Meteor. Soc., 335–337.

Velden, C. S., W. S. Olsen, and B. A. Roth, 1989: Tropical cyclone center-fixing using SSM/I data. *Proc. Fourth Conf. on Satellite Meteorology and Oceanography,* San Diego, CA, Amer. Meteor. Soc., J36–J39.

——, C. M. Hayden, W. P. Menzel, J. L. Franklin, and J. S. Lynch, 1992: The impact of satellite-derived winds and numerical hurricane track forecasting. *Wea. Forecasting,* **7,** 107–118.